AIChE

Phthalic Anhydride Production from Hemicellulose Solutions: Technoeconomic Analysis and Life Cycle Assessment

Zhaojia Lin and Marianthi Ierapetritou
Dept. of Chemical and Biochemical Engineering, Rutgers—The State University of New Jersey, Piscataway, NJ

Vladimiros Nikolakis
Catalysis Center for Energy Innovation and Dept. of Chemical & Biomolecular Engineering,
University of Delaware, Newark, DE

DOI 10.1002/aic.14921

The process synthesis, technoeconomic analysis, and life cycle assessment (LCA) of a novel route for phthalic anhydride (PAN) production from hemicellulose solutions are presented. The production contains six steps including dehydration of xylose to furfural, reductive decarbonylation of furfural to furan, oxidation of furfural to maleic anhydride (MA), Diels-Alder cycloaddition of furan, and MA to exo*−4,10-dioxa-tricyclo[5.2.1.0]dec-8-ene-3,5-dione followed by dehydration to PAN in the presence of mixture of methanesulfonic acid and acetic anhydride (AAN) which is converted to acetyl methanesulfonate and acetic acid (AAD), and dehydration of AAD to AAN. The minimum selling price of PAN is determined to be $810/metric ton about half of oil-based PAN. The coproduction of high-value products is essential to improve the economics. Biomass feedstock contributes to the majority of cost. LCA results shows that biomass-based PAN has advantages over oil-based PAN to reduce climate change and fossil depletion however requires more water usage.* © 2015 American Institute of Chemical Engineers *AIChE J*, 61: 3708–3718, 2015

Keywords: phthalic anhydride, hemicellulose solutions, process design, technoeconomic analysis, life cycle assessment

Introduction

The great economic and environmental incentives have motivated the development of biorefinery as an alternative to refinery, as biomass resources can be used to produce both high-volume, low-value fuels, and high-value chemicals which are projected to contribute 20% of US transportation fuel and 25% of the production of US commodities, respectively in 2030.[1,2] Intensive interests have arisen to develop biobased chemicals. Ethanol, furfural, glycerol and derivatives, levulinic acid, hydroxymethylfufural (HMF), etc. have been identified as top added-value chemical platforms that can be derived from biomass.[3,4] The technology development of these important building blocks can be found in Ref. 4. Furfural, one of these chemicals, has annual global production capacity around 300,000 tons, and it is produced from the hydrolysis of xylan to xylose followed by xylose dehydration.[5] Its industrial production requires treatment of pentosan rich biomass with strong mineral acids and high-pressure steam and suffers from low furfural yields.[5–8] Recently, a new approach with much higher yield has been developed. This process involves the utilization of milder acid hydrolysis, with autocatalysis by acetic acid (AAD) that is coproduced with furfural and formic acid, and integration with extraction to prohibit the production of humins.[6,9,10] Furfural can be exploited to produce a range of important chemicals such as furan, maleic anhydride (MA), tetrahydrofuran (THF), furfuryl alcohol, etc.[7]

A path for converting furfural to phthalic anhydrite (PAN) is another recent discovery.[11] It involves the Diels-Alder cycloaddition of furan with MA followed by dehydration of the cycloadduct.[11] It is envisioned as a potentially renewable route as both furan and MA can be produced from furfural. The renewable reaction routes used in this work are shown in Figure 1. PAN is an important intermediate with annual global production around 3 million tons in 2000, which is mainly employed to manufacture phthalic plasticizers used in the production of flexible PVC conducts, and unsaturated polyester resin and alkyd resin that are for surface coating.[12] Some minor applications include polyester polyols, pigments, dyes, etc.[12] Traditionally, petroleum-based PAN is produced from the catalytic oxidation of *o*-xylene or naphthalene at the range of 593 to 673 K using a modified vanadium pentoxide (V_2O_5) catalyst.[12] The selectivity of PAN is 70% and MA is coproduced with 10% selectivity.[12]

Furan is commercially produced either by the decarbonylation of furfural, or via the partial oxidation of 1,3-butadiene which is produced from the C_4 fraction of naphtha and gas oil cracking.[7,13] Decarbonylation can be achieved by the oxidative decarbonylation in the presence of steam,[14,15] or by the reductive decarbonylation.[16–18] It is noted that the oxidative decarbonylation requires higher temperature resulting in

---

Additional Supporting Information may be found in the online version of this article.

Correspondence concerning this article should be addressed to M. Ierapetritou at marianth@soemail.rutgers.edu

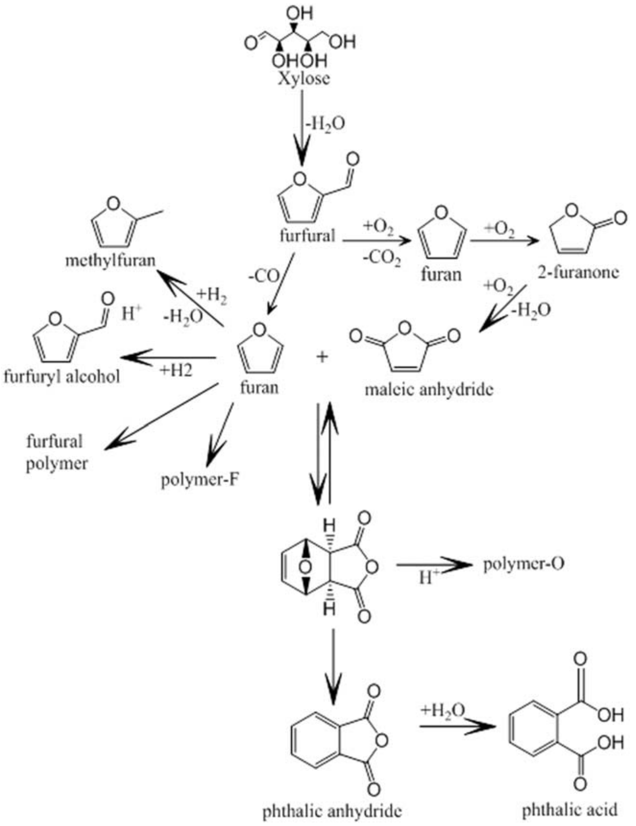

Figure 1. The reaction route for the biobased phthalic anhydride production.

higher utility cost. In comparison, the reductive decarbonylation needs lower temperature and is carried out in either vapor phase with H_2[16–18] or in liquid phase.[19,20] Vapor-phase decarbonylation occurs in presence of H_2 with a supported precious metal catalyst, which has the advantages of high yield, and relatively simple catalyst recycling and regeneration.[16–18] The liquid-phase decarbonylation proposed in Refs. 19 and 20 uses Pd/C catalyst at 423 K, also achieving high yield but requires much longer reaction time (hours). The separation systems for both processes are very similar. Although the reaction temperature in the case of liquid phase reactions is about 150 K lower than that of the vapor phase ones, the latter has the advantage of short residence time (seconds) and inline catalyst regeneration. In this work, the path using reductive decarbonylation with H_2 is selected despite the fact that this might not be the optimum selection.

Industrially, MA is produced by the oxidation of benzene or other aromatic compounds. Lately, vapor-phase oxidation of *n*-butane has started to dominate the industry.[21] MA can also be renewably manufactured from vapor-phase oxidation of furfural.[22–25] High selectivity has been reported in the literature however the catalyst efficiency is very low leading to an extremely small feed stream that can be used. To leverage the MA yield and the catalyst efficiency, the experimental results discovered in Ref. 24 are used in this work.

The commercialization of biobased chemicals is still at an early stage of development. Technoeconomic analysis and life cycle assessment (LCA) are useful tools to facilitate the advancement of new processes, to assess and compare the feasibility of different alternatives, and to determine the most important parameters that have to be improved to promote process commercialization. In detail, LCA provides a systematic procedure designed to compile inventories of energy and material inputs and environment releases, and to assess the overall environmental impacts of a product or a process associated with economic, social, and ecological impacts within the defined domain such as from-cradle-to-grave, from-cradle-to-gate, and from-gate-to-gate.[26] A lot of work has been done related to the C_6 sugar conversion to HMF, levulinic acid, gamma-valerolactone, etc.[27–31] In our previous studies,[29,30,32] we have analyzed the production of biobased *p*-xylene from C_6 sugar and shown that the biobased chemicals are usually more expensive than those from oil sources, but present comparable environmental impacts as oil-based chemicals. The most important components of the cost and environmental impacts come from the cultivation biomass feedstocks and its loss to low value by-products as well as the necessity of the large amounts of solvents. Thus the idea of a biorefinery focusing on the production of high added value products (and byproducts) is very useful to make the production more competitive. The production of PAN offers an alternative to utilize C_5 sugars. However there is limited work in the literature to cover the economic analysis and LCA of the production starting from C_5 sugars, which is the main focus of this work.

In particular, this work aims to design a process for the production of PAN based on a novel path that uses a renewable biomass feedstock and evaluate its technoeconomic potential and environmental burdens. The remainder of the manuscript is structured as follows. The next section presents the methodology containing the detailed descriptions of reaction paths, the process flowsheet, the methods and assumptions of process design and economic analysis, and the details of LCA. In the section of Results and Discussion, we present the main results based on the flowsheet simulation, the economic analysis including sensitivity analysis and LCA.

Methodology

Reaction routes

Furfural Production. Furfural can be produced from xylose using reactive extraction, which leads to much higher yield than that of the current industrial practice (i.e., 55%).[9] The production process developed in Ref. 9 has been implemented in this work. Specifically, furfural is produced in a biphasic reactor having two liquid phases (one water rich and one water depleted phase). Xylose dehydration occurs in the aqueous phase in presence of an acid (i.e., HCl) catalyst. Furfural is extracted to the organic rich phase to minimize losses due to side reactions. THF is used as extractant and NaCl is added in the aqueous phase to promote the partition coefficient of furfural.[9] The highest obtained conversion and selectivity of furfural are 100% and 90%, respectively, at 493 K, 2:1 organic to aqueous phase volumetric ratio, and 0.35 mol/L HCl.[9]

Furan Production. Reductive decarbonylation can be achieved by using either high or low H_2 to furfural ratios.[17,18] In the former case, a 20:1 H_2 to furfural ratio is typically used at 533 K together with K-doped Pd/Al_2O_3 resulting in high furan yields (~99.5%), which leads to longer catalyst lifetime due to the regeneration of the catalysts with H_2.[17] However, such high H_2 to furfural ratio increases the volume of the processing units and causes separation issues of CO, H_2, and furan due to low concentration of furan which is less than 0.05%. In the latter case, a 2:1 H_2 to furfural ratio is used at 573 K with

Pd/Li-aluminate catalysts promoted by cesium carbonate. This might lead to a shorter catalyst lifetime but simplifies the recovery system. The overall yield at 95.2% conversion is ~91% which is slightly lower than that of the high ratio case. However, since recovery of furan is easier the reductive decarbonylation using the low H_2 to furfural ratio is selected. The byproducts include furfuryl alcohol with 3.23% selectivity, and methylfuran with 0.97% selectivity.[18]

Maleic Anhydride Production. MA is converted from furfural via gas phase oxidation, which mechanistically contains three stepwise oxidations—first furfural to furan, then furan to 2-furanone and finally 2-furanone to MA.[24] The products vary depending on the reaction conditions (i.e., temperature and pressure) and catalyst structure. The reaction is assumed to occur at 593 K with 570 kPa O_2 and 150 kPa furfural using VO_x/Al_2O_3 as solid catalysts. The conversion of furfural is 100% and the selectivity of MA is 73%. Neither furan nor 2-furanone were detected under the specific conditions and the only byproduct is the furfural resin.[24] In the simulation, air is used as the oxygen source since the other compositions of air do not participate in the reaction and the usage of air also has the advantage to avoid the explosion.[22,23]

Phthalic Anhydride Production. The previously-produced furan and MA are converted to PAN in two steps. The first step is a Diels-Alder cycloaddition of furan and MA to produce *exo*-4,10-dioxa-tricyclo[5.2.1.0]dec-8-ene-3,5-dione (oxanorbornene dicarboxylic anhydride or ODA) at the room temperature and 170 kPa under solvent-free conditions. The conversion of the furan and MA is 96% and the selectivity of ODA is 100%. Next, the ODA is dehydrated to PAN with 100% conversion in the existence of mixed-sulfonic carboxylic anhydrides in methanesulfonic acid (MSA) at the room temperature. The selectivity of PAN is 80% (not including those that are later converted to phthalic acid (PAD)), while partial amount of PAN is converted to PAD accounting for 7% of ODA. 5% of ODA is under the retro-Diels–Alder reaction to produce MA and furan which is subsequently polymerized to polymer-F, while the rest 95% of ODA is polymerized into polymer-O.[11]

Acetic Anhydride Recovery from Acetic Acid. Mixed-sulfonic carboxylic anhydrides in methanesulfonic acid is used as the solvent in the dehydration of ODA to PAN, which mixes MSA with acetic anhydride (AAN) to generate acetyl methanesulfonate (AMSA) and AAD. At the end of reaction, AMSA is converted back to MSA but AAD is coproduced with reaction proceeding.[11] Given the large amount of AAD produced and the large price difference between AAN ($1885/metric ton[33]) and AAD ($665/metric ton[34]), the dehydration of AAD to AAN has been taken into the consideration. Specifically, the AAD is dehydrated to ketene at a temperature around 973K and total pressure of between 20 and 30 kPa using triethylphosphate as a catalyst. The conversion of AAD is about 80–90% and the selectivity to ketene is about 90–95%. The ketene is then reacted with AAD to form AAN with 99% selectivity at 318–328 K.[35]

Process Design and Simulation

A novel process is designed and simulated to produce PAN based on the aforementioned reaction routes using Aspen Plus® V8.6.[9,11,18,24,35] Most of components involved in the simulation are directly selected from Aspen database, while the compounds that are not included in the database are defined by their molecular structure with the properties estimated by ThermoData Engine that corresponds to a thermodynamic data correlation, evaluation, and prediction tool developed by the National Institute of Standard and Technology and implemented in Aspen Plus.[36,37] More specifically, ODA, MSA, and AMSA are defined by their structure. The solid formation enthalpy and the solid heat capacity of ODA are estimated as 10.97 kJ mol^{-1} and $139.07 + 9.65 \times T$ J mol^{-1} K^{-1} using two different functional group methods developed in Refs. 38 and 39, correspondingly. Those compounds with no specific molecular structure or complex structure are specified by the surrogates, for example polymer-O (polymer of ODA) and polymer-F (polymer of furan) are assumed as $C_8H_6O_4$ and $C_8H_8O_2$ based on the compositions of C, H, and O elements in Ref. 11 which are the solid surrogates of PAD and methyl-benzoate. The NRTL method is utilized to predict the liquid-liquid and liquid-vapor behavior of the main units while the ideal method is employed to calculate the energy balance for the mixers, splitters, and filters. The missing binary parameters in NRTL model are estimate using the UNIFAC method.[36] The behavior of extraction is estimated by user-supplied partition coefficients from the preliminary experimental results. The reaction and separation stages have not been optimized given the fact that there is limited knowledge regarding the optimum reaction conditions, and the identification and utilization of byproducts.

Furthermore, the following assumptions are made to design and simulate the production process:

1. The inlet streams of furfural for the production of furan and MA are adjusted to ensure the appropriate molar amounts of furan and MA required for the production of PAN.
2. The H_2 molar ratio to furfural is fixed at 2:1 in the production of furan.
3. The flow of air stream fed into the MA production section is adjusted to ensure that the O2 molar ratio to furfural is 3.6:1.
4. Considering the complexity of the separation of H_2 and CO, the mixed syngas (primarily consisting of H_2 and CO) from the furan production is assumed as the raw material for other synthesis processes which can be used to produce several chemicals such as oxo alcohols, methanol or synthetic fuel.
5. The molar ratio of MSA to AAN to PAN is selected from[11] as 39:26.4:6.02.
6. Toluene is used to extract PAN or PAD from the product mixtures containing solvents of MSA and AMSA. The volumetric ratio of toluene to the product stream is selected as 2:1.[11]
7. As the crystallization rates of PAN or PAD and polymer-O are not known, the surrogate model is approximated by a liquid-to-solid reactor, which only takes into consideration the overall percentage of liquid that is crystallized to solid. The default value of solid size is used as 0.83 mm and the crystallization rate is assumed as the flow rate of the solid components.

Process Flowsheet

The process flowsheet is shown in Figure 2 including six sections. Section 100 represents to the furfural production from xylose which is based on the process flowsheet proposed in Ref. 9. Hemicellulose solution containing makeup sodium chloride and HCl (stream 1) is mixed the recycled HCl (stream 6) and sodium chloride (stream 9) enters the biphasic reactor (101). The makeup THF solvent (stream 2) and recycled THF

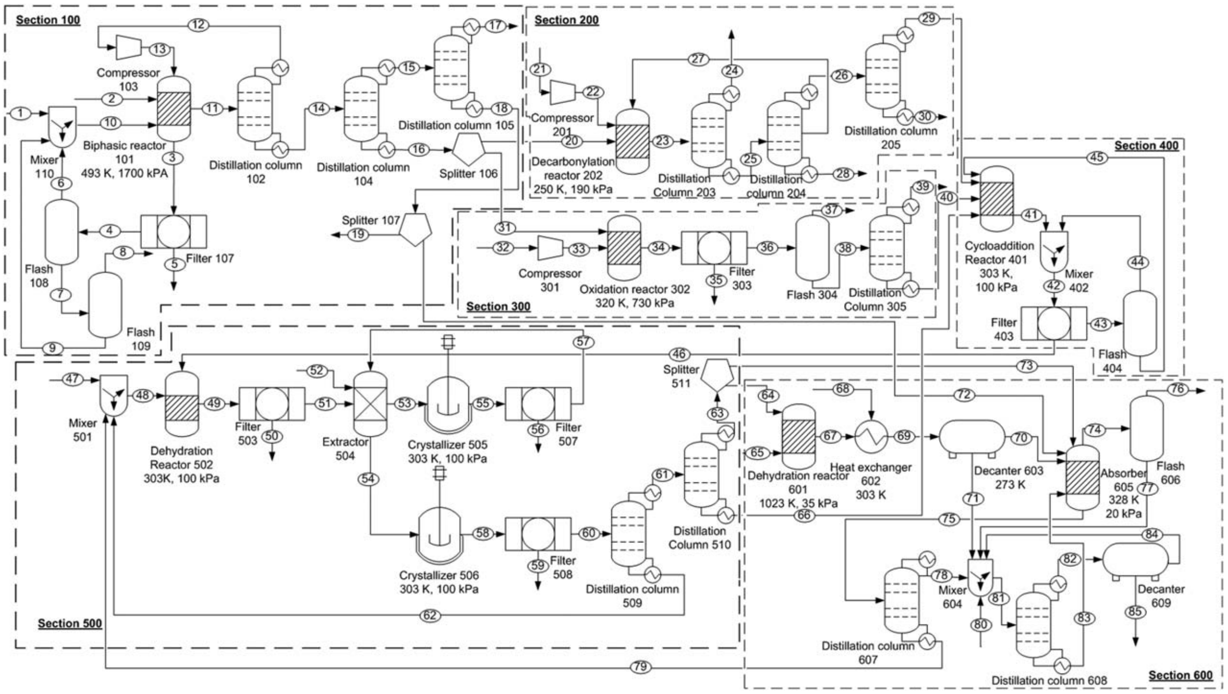

Figure 2. The process diagram: Section 100—furfural production, Section 200—furan production, Section 300—maleic anhydride production, Section 400—ODA production, Section 500—phthalic anhydride production, and Section 600—recovery of acetic acid.

(stream 13) are used as extractant solvent. The organic phase (stream 11) of the biphasic reactor (101) mainly contains THF, furfural, formic acid, and AAD. A THF distillation column (102) is used to separate the THF to recycle. Stream 13 connects to a furfural distillation column (104) where furfural (stream 16) is obtained from bottom and the top stream 15 is fed to another distillation column (105) to separate formic acid (stream 17) and AAD (stream 18).[9] The aqueous phase (stream 3) connects to a filter (107) to remove humins (stream 5) and the solutions (stream 4) is fed to a flash drum (108) to recycle most of HCl (mixed with water) (stream 6). The bottom stream 7 is connected to a flash drum (109) to evaporate most water to recycle sodium chloride (stream 9).

Section 200 contains the production of furan from furfural. Furfural (stream 20) mixed with H_2 (stream 21) enters into the decarbonylation reactor (202) to be converted to furan at 573 K and 172 kPa. The product stream 23 then connects to a distillation column (203) to remove the low boiling compounds such as H_2 and CO (stream 24). The distillation column is selected to separate furans from H_2 and CO so that they can be used as syngas to participate in the other synthesis process without the need of other purification. The heavy stream 25 connects to a distillation column (204) to recover and recycle any unreacted furfural (Stream 27) and to remove the furfuryl alcohol (stream 28). The distillate (stream 26) enters another distillation column (205) that produces pure furan (stream 29) in the top. The bottom stream 30 mainly contains methylfuran and water. Section 300 involves the production of MA from furfural. Air (stream 32) is compressed into the oxidation reactor (302) and mixed with furfural (stream 31) to produce MA. The product stream 33 enters a filter (303) to remove the polymer of furfural (stream 35). The liquid stream 36 is then fed to a flash (304) to remove N_2, CO_2, and unreacted O_2. The remaining water is removed in a distillation column (305) to obtain pure MA.

ODA is manufactured in Section 400. Furan (stream 29) and MA (stream 40) mixed with recycled furan and MA (streams 45 and 66) enter the cycloaddition reactor (401). Stream 41 is washed with furan (stream 44) and connected to a filter (403) to purify the ODA (stream 46). The liquid phase (stream 43) connects to a flash (404) to split into washing furan (stream 44), and unreacted furan and MA (stream 45). Section 500 includes the dehydration of ODA to PAN. Solvent MSA (stream 47) is mixed with AAN (stream 79) and recycled MSA and AMSA (stream 62) in a mixer (501) to generate AMSA and AAD which is then fed to the dehydration reactor (502) with ODA (stream 46) to produce PAN where AMSA is converted back to MSA and AAD. The coproducts include MA, polymer-O and polymer-F. Polymer-F exists as the solid in the stream 49 and is removed via a filter (503). Then toluene (stream 52 and 57) are added to extract the PAN and PAD from the main effluent (stream 51). The toluene rich phase (stream 53) mainly containing the PAN and PAD enters a crystallizer (505) and a filter (507) to achieve pure PAN (containing a small amount of PAD) (stream 56). The MSA-rich phase (Stream 54) first enters a crystallizer (505) followed by a filter (508) to remove the polymer-O (stream 59). The liquid phase (Stream 60) is then fed into a distillation column (509) to recycle MSA and AMSA (stream 62). The top stream 61 enters another distillation column (510) to separate AAD (stream 63) and MA (stream 66).

AAN is recovered from AAD at section 600. AAD (stream 64) enters the dehydration reactor (601) to be converted into ketene. The reaction occurs at a temperature around 973K and pressure of 30 kPa using triethylphosphate (stream 65) as a catalyst. Ammonia (stream 68) is added at the heater (602) exit to avoid the reverse reaction. A slightly excess of ammonia generates acetamide acting as a ketene polymerization inhibitor in the recovery step. The mixed stream is then fed to a decanter (603) at 273K to generate ketene rich phase (stream

Table 1. Summary of Investment Parameters

Name	Characterization
Operating mode	Continuous; 8000 h/year
Economic life	20 years
Internal rate of return (ROR)	15%
Escalation rate	3.5%
Tax rate	35%
Salvage value	10%
Depreciation method	Straight line
Working capital percentage	5%
Plant overhead	50%
G and A expense	8%

70) and water rich phase (stream 71). Ketene rich phase is absorbed by and reacted with AAD (stream 72 and 73) to form AAN with 99% selectivity at an absorber (605). The cooling of the absorber is useful to avoid the side reactions such as ketene polymerization. The top stream 74 connects to a flash (606) to remove methane and CO_2 (stream 76). Bottom stream 68 from the absorber (605) containing about 90% AAN with excess AAD, are separated using a distillation column (607). The top stream 78 mixed with stream 71, 77, and 84 enters an azeotropic column (608) using ally ester (stream 80) as the azeotropic solvent to remove water (mixed with ally ester). A decanter (609) is employed to remove water from ally ester.[40]

Economic Analysis

Aspen Economic Analyzer® V8.6 is employed to estimate the equipment and operating costs of PAN production which are based on the quotes of first quarter in 2013.[41] The discounted cash flow analysis is then used to determine the minimum cost of PAN which is defined as the selling price of the product when the net present value is zero.[42] The capacity of the plant is 132.6 kton PAN per year, which is based on the largest capacity of the PAN plant in United States.[43] The assumed capacity requires the use of 551.4 kton (dry basis) hemicellulose solution per year roughly that needs 1593 kton biomass feedstocks. A paper mill plant is one possible source of the required hemicellulose quantities.[44] Furthermore, the total annual biomass resources available in the United States are roughly 423 million ton.[45] Therefore, if further developments in the area of biorefinery are implemented a standalone plant with capacity of 132.6 kton/year can also be considered as realistic long-term alternative. In any case the impacts of plant capacity on the economics are addressed using sensitivity analysis.

The investment parameters implemented in this work are listed in Table 1 while the raw materials' cost is summarized in Table 2. The production of hemicellulose solutions using dilute acid hydrolysis has been previously examined in our work.[32] The economic analysis is based on the capital cost reported in Ref. 46 and scaled to first quarter of 2013 and capacity using in our simulation. The burning heat from lignin is used to coproduce heating steam that is needed in the hydrolysis process and excess electricity that can be sold to the grid. One ton biomass feedstock can be used to produce 0.346 ton (dry basis) of hemicellulose, 0.211 ton (dry basis) of glucose, and 0.187 kwh of electricity. The biomass feedstock is assumed as \$80/ton.[47] The capital cost is determined \$785 million from which the total installed equipment is \$432 million accounting for 55% of the capital cost. The operating cost is estimated as \$122 million/yr. The glucose price is fixed at \$300/ton and the excess electricity is \$0.0688/kWh so that the hemicellulose solution is determined as \$135/ton.[46] This number is very close to \$130/ton of xylose which is derived from pre-processing extracts at an integrated forest products refinery at a hardwood mill.[9] The syngas mixture including H_2 and CO is considered the same value of natural gas which is averaged to \$3.79/GJ with heating value as 53.5 GJ/metric ton[48]; thus the syngas is \$203/metric ton. The price of AAD varied from about \$650 to 1000/metric ton during the last 10 years span[34] and the current price is at the bottom of that range. The value of polymer of furfural, polymer-O and polymer-F are unknown thus not included for the base scenario.

The catalyst cost is estimated as precious metal cost plus \$11,000/ton of supported catalyst and catalyst manufacturing.[27] The Pd/Li-aluminate catalyst that is used in the conversion of furfural to furan consists of 0.5 wt % Pd with the unit price of \$28614/kg,[49] leading to the unit price of Pd/Li alluminate is \$154,000/ton. The total amount of catalyst is estimated based on the bench-scale data and obtained as 2.04 ton/charge.[18] The VO_x/Al_2O_3 catalyst used for the MA production is \$11,000/ton. The amount is extrapolated from the available information in Ref. 24 and calculated as 30.60 ton/charge. It is assumed that the deactivation of catalysts is caused by the production of coke. The coke on the catalyst is burned off at a temperature around 783 K.[50–52] Exact information about the catalyst stability on stream is not known; however, based on the literature Pd/Li-aluminate and VO_x/Al_2O_3 remain active for at least 116 h and 12 h, respectively.[18,24] The catalyst regeneration usually takes 5 h.[50–52] Therefore continuous regeneration of catalysts is assumed at 783 K though the regeneration temperature highly depends on the reaction conditions, coke composition etc. Two reactors are assumed to operate in parallel one for conversion and one for catalyst regeneration. The heating needed in the regeneration of the catalysts is provided by the combustion process of the hydrocarbons formed in the reaction. The overall catalyst life is usually between 6 to 24 months and hereby assumed to be 6 months based on the conservative estimation.[50–52] 99% of precious metals are assumed to be recovered so that 1% of makeup metal and the catalyst support and manufacturing cost are required every six months. Thus the capital cost of Pd/Li-aluminate catalyst is \$0.628million and the operating cost is \$93.23 k/year while the capital cost of VO_x/Al_2O_3 is \$0.673 million and the operating cost is \$1.26 million/year.

Transportation cost and wastewater treatment have not been included. Sensitivity analysis is utilized to assess the uncertainties resulted from the assumptions related to raw materials

Table 2. Summary of Raw Materials Cost and Byproducts

Compounds	Price (\$/ton)
Hemicellulose solution	135 (dry basis)
NaCl	100[44]
THF	1500[44]
HCl	115[26]
Hydrogen	653[26]
MSA	3000[44]
Toluene	1070[45]
Ally ester	5250[44]
Syngas	203[42]
Furfuryl alcohol	1500[44]
Formic acid	1200[9]
Acetic acid	665[32]

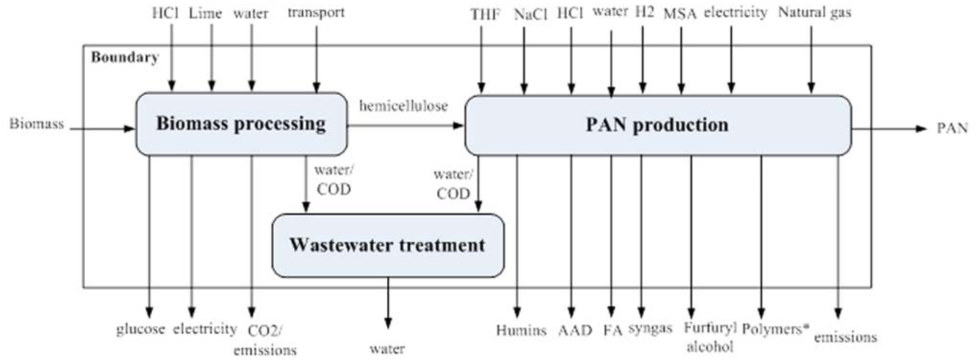

Figure 3. Scope definition of bio-based PAN production process.

***polymers contains polymer of furfural, polymer-O, and polymer-F. [Color figure can be viewed in the online issue, which is available at wileyonlinelibrary.com.]**

cost and the byproducts selling price as well as to address the effect of reaction conversion and selectivity.

Life Cycle Assessment

The goal of LCA is to evaluate the environmental burdens of the biobased PAN production from lignocellulosic biomass, understand the most important impacts and finally compare with oil-based PAN production. The scope of system is defined from-cradle-to-gate, shown in Figure 3. One metric ton of PAN is selected as the functional unit to compare the LCA results of different alternatives. Although the LCA can vary intensively with different biomass feedstocks, the wood residue is used as a representative case to illustrate LCA involving two scenarios. One scenario uses wood chips from oak followed by dilute acid hydrolysis from the wood sources in Illinois where the annual available wood is greater than 2000 kton.[45] The biomass processing utilizes dilute acid hydrolysis and the detailed descriptions and the input and output inventory can be found in Ref. 32. The other scenario starts with hemicellulose solutions from paper mill which are often burnt to produce heat. Since the hemicellulose solutions from paper mill are taken to produce furfural, additional energy sources will needed to provide heat. Therefore, the environmental impacts of the hemicellulose solutions from paper mill is considered to be equal to the environmental impacts of addition heating sources that is specified as burning heat from wood chips. To calculate the amount of burning heating hemicellulose, the heating value of hemicellulose (xylose) is assumed 15.67 MJ/kg.[53]

SimaPro V8.0.4[54] is utilized to perform LCA since it involves a broad international-scope life cycle inventory databases and a variety of impact assessment methods. It is known that the life cycle inventory (LCI) varies on different databases due to location, technologies, emission level, etc., but no comparisons between different databases have been included. All datasets are retrieved from Ecoinvent v3.0[56] to avoid issues related to database compatibility. Ecoinvent is the largest database and its LCI has been undergone review and validation with consideration of uncertainties and it contains all datasets used in the process.[55] ReCiPe midpoint method v1.11 is selected in this work. Midpoint method is a traditional cause-effect chain approach of an impact categories with fewer uncertainties.[57] Economic allocation has been applied to share environmental impacts among multiple products using the weighting fraction of the sum of the product values.

In addition, some assumptions are made to perform LCA including:

1. Only the raw materials and solvents are included while the construction and infrastructure materials and catalysts are assumed to be recycled at the end of the lifetime of the project and excluded from the scope. The labor needed in the construction is neither included.
2. Feedstock is transported from the local biomass sources; more specifically the plant is assumed in the middle of Illinois. The assumed capacity (1685 kton) accounts for 5.96% of the annual available biomass resources in Illinois (28284 kton).[45] The biomass resources are assumed evenly distributed so that the average transportation distance between biomass resources to biorefinery facility is 121 km.
3. Electricity is supplied by medium voltage grid based on the average transformation technology and the average electricity loss during transmission in US. Cooling is supplied by water, cooling, unspecified natural origin based on the assumptions that 99.5% of cooling water is recycled and waste heat is emitted into atmosphere.

Results and Discussion

Simulation

The proposed process provides an alternative to produce PAN starting from hemicellulose—one of the main compositions of lignocellulosic biomass feedstock. The summary of flow rates is listed in Supporting Information Table SI1. The overall amount of xylose (dried basis) needed is 551.4 kton/year as well as 4.3 kton/year of H_2, which yields 132.6 kton/year PAN and PAD. The byproduct stream includes 133.4 kton/year of AAD, 33.4 kton/year of syngas, 47.7 kton/year of formic acid, 3.5 kton/year of furfuryl alcohol, 33.4 kton/year of polymer of furfural, 14.6 kton/year of polymer-O, and 4.7 kton/year of polymer-F. The production of PAN from biomass feedstock involves gas, liquid and solid phases; thus it requires a number of different separation units including flash, distillation column, decanter, crystallizer, filter, and extractor. In addition it also requires a large amount of solvents such as THF and MSA.

The production of PAN (Section 400 and 500) can also start with the petroleum-based production of MA and furan. The petroleum-based furan can be produced from C_4 such as 1-butene, 2-butene, and 1,3-butadiene in either vapor phase[58,59] or liquid phase.[60,61] The vapor phase processes are generally characterized by low conversion and selectivity due to the instability of furan compounds at high temperatures in the

Table 3. Summary of Capital Cost

Name	Million $	Percentage
Purchased equipment	148.97	33.00%
Initial catalyst	1.30	0.29%
Equipment setting	0.80	0.18%
Piping	124.49	27.57%
Civil	3.69	0.82%
Steel	0.85	0.19%
Instrumentation	7.56	1.67%
Electrical	1.82	0.40%
Insulation	4.82	1.07%
Paint	0.30	0.07%
Other*	67.96	15.05%
Subcontracts	0.00	0.00%
G and A overheads	10.46	2.32%
Contract fee	9.60	2.13%
Escalation	0.00	0.00%
Contingencies	68.87	15.25%
Total project cost	451.48	100.00%

*Other contains design, engineering, and procurement costs; material charges (freight and taxes); and construction field indirect costs (fringe benefits, burdens, consumables/small tools, insurance, equipment rental, field services, field office construction supervision, and plant start-up)

presence of oxygen which leads to the formation of resinous compounds and uncontrolled polymerization with tars.[58,59] In comparison, the production in liquid phase can lead to much higher selectivity; for example, the reaction of butadiene to furan can achieve up to 99% of selectivity of furan with 13.2% conversion in presence of $Ru_3(CO)_{12}/(n\text{-}C_4H_9)_3GeI$ catalyst based on the results that selectivity is maximized.[61] The subsequent separation of pure furan from unreacted butadiene and solvent (i.e., chlorobenzene) can be achieved using a condenser and a distillation column. The industrial production of MA starts with petroleum source specifically either benzene or *n*-butane at 393–423 K.[21] The process includes following steps—catalytic packed bed reaction to MA, MA conversion into maleic acid using an adsorption tower, and then maleic acid dehydration back to MA. Finally, pure products are achieved by a distillation separation. This petroleum-based production achieves lower yield than the biobased alternative. In addition the raw materials of petroleum alternative such as butadiene and butane vary dramatically with different season. For example butadiene price increased from $850 to $1468 over the last year.[62] In summary, such petroleum-based alternative present worse performance than the biobased alternative in terms of overall yield and raw materials cost.

Economics

Heat integration has also been performed using Aspen Energy Analyzer v8.6. The capital costs are listed in Table 3. The total capital cost is estimated at $451.48 million including heat exchangers used to achieve heat integration. It is noted that equipment purchase accounts for 33.0% of the total capital cost, while the initial charge of the catalysts contributes less than 0.29%. The detailed equipment cost of each unit is shown in Supporting Information Table SI2. The total purchased equipment cost is estimated at $148.97 million where 41.4% of it comes from the heat exchangers required for the production and heat integration including condensers and reboilers. The second largest contributor is from purchased equipment (excluding the heat exchangers) in section 100 namely the dehydration of xylose, accounting for 30.3%. The reason of such high contribution of section 100 is that the dehydration of xylose uses dilute solution (10.7% xylose) to improve selectivity and moreover the 2:1 THF to aqueous phase volumetric ratio further increases the volume of the system.[9] The combination of acid and salts requires the equipment materials at the section 100 to be an expensive acid and salt resistant metal alloy. Another significant contributor is the equipment cost from section 500 accounting for 7.5% since this section also involves the usage of solvent eventually leading to about 10% PAN solution and requires complex separation processes including distillation, extraction, crystallization, and filter.

The total operating cost with the consideration of heat integration is summarized in Table 4. The total operating cost is $151.34 million/year which mainly comes from the raw materials cost accounting for 70.47%. More specifically, the biomass feedstock (hemicellulose solution) accounts for 69.79% of raw material cost, while the makeup solvent THF that is used in the dehydration of xylose and MSA that is employed for the conversion of PAN from ODA account for 10.1% and 9% of total raw materials cost, correspondingly. Although dilute solutions are often useful to obtain high conversion and selectivity, they result in increasing operating cost due to the costs from makeup solvents and utility consumption. Furthermore, it results in increasing capital cost due to the increasing volume of units. H_2 contributes about 2.64% of the total operating cost. H_2 is produced from nonrenewable natural gas; however, it does not participate in the main reaction (may participate in the side-reactions) and at the end of the production it is mixed with CO to supply as syngas. It is certain that with the increasing H_2 price, its contribution will become more significant so it may be necessary to consider the separation of CO and H_2 at that circumstance. The separation of CO and H_2 can be achieved by condensation, distillation, or adsorption however requiring cryogenic temperature. Membrane separation of CO and H_2 has been extensively studied for some decades and has been effectively recover CO and H_2 to relatively high purity. In case that H_2 has to be recycled for due to economics, H_2 can be obtained using the water gas shift of CO with steam to produce CO_2 and H_2 followed by the separation using a pressure swing adsorption.[63]

The total utility cost contribute 12.79% of the operating cost using heat integration which helps to reduce about 81.8% of original heating consumption cost. The utility consumptions contain 88.0 GJ/h of fuel heat, 1632.9 GJ/h of cooling water, 4.3 GJ/h of cooling refrigerant, and 37.8 GJ/h of electricity. The PAN is estimated as $810/metric ton which is about 53% lower than the market price of PAN from petroleum source that is roughly $1706/metric ton.[64] If furfural is directly purchased from market, the price of PAN will increase dramatically. Because of the availability of inexpensive biomass feedstock and new conversion technology of xylose to furfural that obtains much higher yield, the relative inexpensive

Table 4. Summary of Operating Cost

Name	Million $/yr	Percentage
Total raw materials cost	106.65	70.47%
Catalyst cost	1.35	0.89%
Total utilities cost	19.35	12.79%
Operating labor cost	2.04	1.35%
Maintenance cost	6.15	4.06%
Operating charges	0.51	0.34%
Plant overhead	4.08	2.69%
G and A cost	11.21	7.41%
Total operating cost	151.34	100.00%

Table 5. Summary of Product Sale

	Million \$/year	Percentage
PAN	107.44	40.49%
Furfuryl alcohol	5.25	1.98%
Syngas	6.78	2.56%
Formic acid	57.22	21.56%
Acetic acid	88.68	33.42%
Total product sale	265.37	100.00%

biobased PAN can be obtained based on the production process presented in this work.

The annual production sale is summarized in Table 5. The revenue comes from the product sale including the sale of PAN, the sale of furfurl alcohol, the sale of syngas, and the sale of AAD and formic acid that are produced in the conversion of furfural from xylose. It is noted that 40.49% of revenue comes from the sale of PAN, 33.42% is from the sale of AAD, and 21.56% corresponds to the sale of formic acid.

Sensitivity analysis

The price of different chemicals varies with the location, season, etc.; therefore, the sensitivity analysis is performed to assess the impacts of the price variability of raw materials, coproducts, and plant capacity. Heat integration is taken into account for all the scenarios. The results are shown in Figure 4. The base scenario is set as 100%, while the scenarios labelled as 25%, 50%, and 200% correspond to their percentage of the base scenario. 25% of current xylose price can reduce the PAN price by 52% while twice the xylose price will increase PAN price to \$1371/metric ton. The impact of AAD price is dramatic so that 200% of current AAD price will drop PAN by \$142/metric ton while 200% of current formic acid price will decrease PAN to \$379/metric ton. The impacts of other raw materials and byproducts are small. The value of polymer-O, polymer-F, and polymer of furfural is not included while if they can be valued at \$500–1500/metric ton then the PAN minimum price can be reduced by \$199 to \$596/metric ton. 25% of the plant capacity of the base scenario which is 33.25 PAN kton/year raises PAN price by about 24.7%. 50% of plant capacity results in 5.7% increase of PAN price. Doubling the plant capacity decreases the PAN price by 4.0% which indicates that the selected capacity is near the optimal region.

In addition, the sensitivity analysis is employed to determine the impacts of reaction parameters such as selectivity and conversion on the total cost to direct the further research to improve the alternatives. 5% variation of conversion and selectivity is considered for most reactions in order to ensure the same separation units can still be used to achieve the same purity. The results are shown in Figure 5. For those already with high selectivity and conversion, only the negative variation is considered. Moreover, the reduction of the selectivity of ODA conversion is not considered given that the potential byproducts are not known and this will affect greatly the separation process. Increasing selectivity of furfural production from xylose can effectively reduce the PAN price by 2.46%. Decreasing selectivity of furan from furfural decreases the minimum PAN price since the value of the byproduct—furfuryl alcohol (\$1500/ton) from the furan production is considered. It indicated that the production of high-valued products is essential to improve the economics of production. If the conversion of ODA to PA is reduced, then unreacted ODA is mixed with polymer-F and removed by the filter FL3, which leads to a great loss of ODA and substantially increases the cost. The variation of the conversion of the remaining reactions results in small changes on the overall price between 1.0% and 1.7% because the unreacted materials are mostly recycled. In the case of decreasing conversion of MA from furfural, a side stream is connected to the distillation column 305 to recycle furfural that contains a small amount of water and a small amount of furfural is lost with water from the distillate. Thus a slightly higher variability is detected for conversion of furfural to MA. In comparison the selectivity change usually has bigger impact than conversion variation. It is noted that the negative decrease has much higher impact than the positive variation due to increasing separation and recycling costs. The selectivity reduction of MA from furfural increases the need of furfural stream and larger utility consumptions of air. The reduction of selectivity of ODA to PAN leads to more MA increasing the recycling cost and the loss of recycling stream.

Table 6. Characterization Results of Climate Change, Water Depletion and Fossil Depletion

Impact Category	Unit	Oak	Papermill	Oil
Climate change	kg CO_2 eq	6.3E+02	8.1E+02	2.6E+03
Water depletion	m3	2.0E+01	1.4E+01	1.3E+01
Fossil depletion	kg oil eq	1.9E+02	2.0E+02	1.6E+03

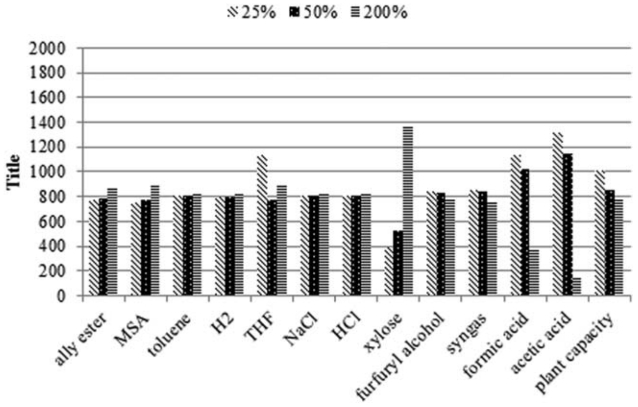

Figure 4. The minimum price of phthalic anhydride with the variation of raw materials, byproducts, and plant capacity.

LCA results

The production starting with biomass feedstock is mainly to solve two concerns that are depleting fossil fuels and

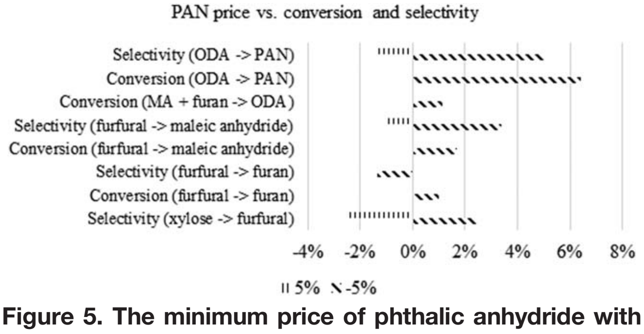

Figure 5. The minimum price of phthalic anhydride with the variation of conversion and selectivity.

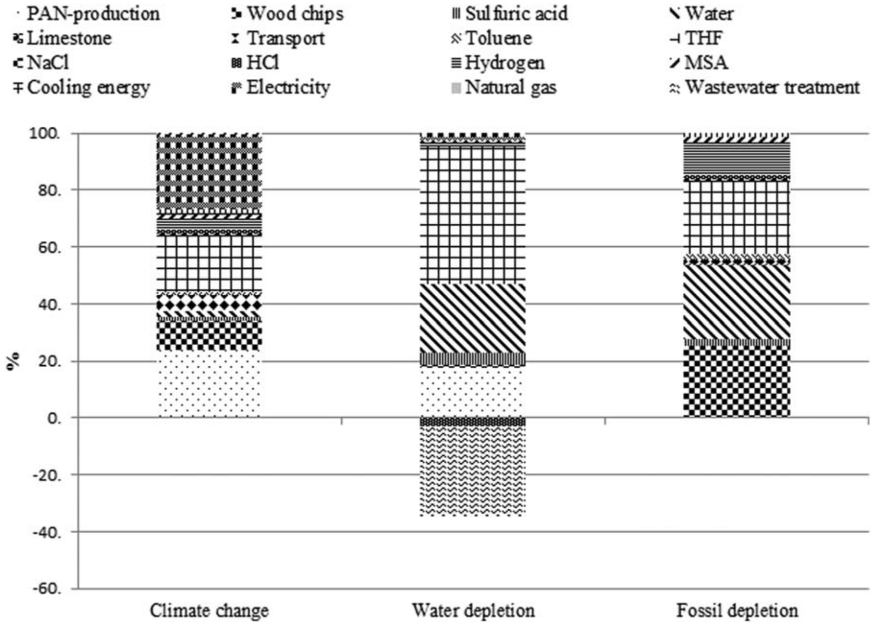

Figure 6. Contribution of selected categories of PAN from oak chips using ReCiPe midpoint method.

increasing greenhouse gas emission. Therefore, the characterization results including climate change, water depletion, and fossil depletion are discussed in detail. The characterization results of biobased PAN starting with oak chips (Oak), with hemicellulose solutions from paper mill (Mill) and oil-based PAN (Oil) using ReCiPe Midpoint method are shown in Table 6. A complete set of results including all the impact categories are shown in the Supporting Information Table SI3. It is noted that PAN from oak chips and paper mill is useful to correspondingly reduce 75.8% and 68.8% climate change (as expressed as kg CO_2 emissions eq.) of oil-based PAN. PAN from oak chips and paper mill can also prevent fossil depletion (as expressed as kg oil eq.), and it results in the 11.9% and 12.5% of fossil depletion comparing to oil-based PAN, correspondingly. However, the production of biomass has worse performances in the categories of water depletion. It requires 153.8% and 107.7% of water needed in oil-based PAN since the production starting with biomass feedstocks uses dilute system to improve selectivity and conversion, which rises the consumptions of water intensively and may improve using water exchange network.

The detailed contribution of the selected category including climate change, water depletion, and fossil depletion of oak-based PAN is shown in Figure 6 and the detailed results of different impact categories are shown in Supporting Information Figure SI. The climate changes or CO_2 emission is mainly from CO_2 emitted from PAN production process, electricity used in PAN and makeup solvent THF. Makeup solvent THF production also contribute significantly for water depletion. The fossil fuel depletion is caused by the production of deionized water, makeup THF, and the cultivation and processing of woodchips.

Conclusions

With the increasing attention on biobased chemicals, it is of great importance to perform technoeconomic analysis and LCA on alternative production routes to assess them from a process viewpoint leading to the development of biorefinery. This work focuses on the process design and evaluation on the production of PAN from biomass-derived hemicellulose solutions which contains the following steps—dehydration of xylose to furfural, reductive decarbonylation of furfural to furan, oxidation of furfural to MA, Diels-Alder cycloaddition of furan and MA to ODA and dehydration of ODA to PAN. The values of byproducts except of the polymers are involved. The consideration of heat integration leads to the minimum price of PAN as \$810/metric ton, which is much lower than petroleum-based PAN. To produce one ton of PAN as well as 1.01 ton of AAD and 0.36 ton of formic acid, 4.16 ton (dry basis) of 10.7 wt % xylose solution and 0.36 ton of natural gas (if the conversion efficiency is assumed as 0.7 and the composition of natural gas is methane) are required. Therefore, the 86% of the PAN carbon is from renewable biomass and 14% from natural gas.

Raw materials from biomass feedstock dominate the operating cost. The use of dilute carbohydrate solutions and extraction solvent increases the operating cost (specifically raw materials cost) as well as the capital cost. The PAN production from ODA requires lower reaction temperature and pressure than oil-based route, which is useful in terms of energy savings. However, the use of solvent and the existence of gas, liquid, and solid phases increase the complexity of separation process. Since most of the reactions have already high conversion and/or selectivity, sensitivity analysis is only performed on those eligible to vary. In general, high selectivity is favored as it has more impact on the process economics. The coproduction of high-value products is very useful to improve the economics of the system. The increasing price of formic acid and AAD is very useful to decrease selling price of PAN. The assumed plant capacity is near the region of the optimum; thus the small positive variance of capacity has fewer impacts than the decreasing capacity. LCA indicate that biomass-based PAN production has reduced impacts of climate change and fossil depletion; however it has raised the needs of water.

To further understand the design of the separation system, more studies are required to understand extraction and crystallization to provide more accurate crystallization rate and partition coefficients. Alternative extraction solvents can be studied which may have better performance than toluene. The replacement of the electricity source from natural gas or coal to renewable one will further reduce the overall environmental impacts. Additionally, great amounts of THF that are required in the dehydration of xylose have large impacts on some of the categories. Biobased production is at the early stage development of technology; hence, with the integration of biomass conversion to fuels, chemicals, electricity, etc., it will become more environmentally friendly.

Acknowledgment

This work was financially supported from the Catalysis Center for Energy Innovation, an Energy Frontier Research Center in University of Delaware funded by the U.S. Department of Energy, Office of Science, Office of Basic Energy Sciences under Award Number DE-SC0001004.

Literature Cited

1. Bozell JJ. Feedstocks for the future—biorefinery production of chemicals from renewable carbon. *CLEAN–Soil, Air, Water*. 2008; 36(8):641–647.
2. Perlack RD, Wright LL, Turhollow AF, Graham RL, Stokes BJ, Erbach DC. *Biomass as Feedstock for a Bioenergy and Bioproducts Industry: The Technical Feasibility of a Billion-Ton Annual Supply*. Springfield, VA, United States Department of Energy, 2005.
3. Bozell JJ, Hollada JE, Johnson D, White JF. *Top Value-Added Chemicals from Biomass. Volume II—Results of Screening for Potential Candidates from Biorefinery Lignin*, Richland, WA, Pacific Northwest National Laboratory, 2007.
4. Bozell JJ, Petersen GR. Technology development for the production of biobased products from biorefinery carbohydrates-the US Department of Energy's "Top 10" revisited. *Green Chem.* 2010;12(4):539–554.
5. De Jong W, Marcotullio G. Overview of biorefineries based on co-production of furfural, existing concepts and novel developments. *Intl J Chem React Eng*. 2010; 8(1), pp. -. Retrieved 2 Jul. 2015, from doi:10.2202/1542-6580.2174
6. Cai CM, Zhang T, Kumar R, Wyman CE. Integrated furfural production as a renewable fuel and chemical platform from lignocellulosic biomass. *J Chem Technol Biotechnol*. 2014;89(1):2–10.
7. Hoydonckx HE, Van Rhijn WM, Van Rhijn W, De Vos DE, Jacobs PA. Furfural and Derivatives. *Ullmann's Encyclopedia of Industrial Chemistry*, Wiley-VCH Verlag GmbH, Weinheim 2000.
8. Lange J-P, van der Heide E, van Buijtenen J, Price R. Furfural—a promising platform for lignocellulosic biofuels. *ChemSusChem*. 2012;5(1):150–166.
9. Xing R, Qi W, Huber GW. Production of furfural and carboxylic acids from waste aqueous hemicellulose solutions from the pulp and paper and cellulosic ethanol industries. *Energy Environ Sci*. 2011; 4(6):2193–2205.
10. Chheda JN, Roman-Leshkov Y, Dumesic JA. Production of 5-hydroxymethylfurfural and furfural by dehydration of biomass-derived mono- and poly-saccharides. *Green Chem*. 2007;9(4):342–350.
11. Mahmoud E, Watson DA, Lobo RF. Renewable production of phthalic anhydride from biomass-derived furan and maleic anhydride. *Green Chem*. 2014;16(1):167–175.
12. Lorz PM, Towae FK, Enke W, Jäckh R, Bhargava N, Hillesheim W. Phthalic Acid and Derivatives. *Ullmann's Encyclopedia of Industrial Chemistry*: Wiley-VCH Verlag GmbH, Weinheim 2000.
13. Dahlmann M, Grub J, Löser E. *Butadiene. Ullmann's Encyclopedia of Industrial Chemistry*: Wiley-VCH Verlag GmbH, Weinheim 2000.
14. Whitman GM, Inventor; Du Pont, assignee. Method of preparing furan, US patent US 2374149 A,1945.
15. Coca J, Morrondo ES, Sastre H. Catalytic decarbonylation of furfural in a fixed-bed reactor. *J Chem Technol Biotechnol*. 1982;32(7–12): 904–908.
16. Manly DG, O'halloran JP. Inventors; US3223714 A, assignee. Process of producing furan, 1965.
17. Zhang W, Zhu Y, Niu S, Li Y. A study of furfural decarbonylation on K-doped Pd/Al2O3 catalysts. *J Mol Catal A: Chem*. 2011;335(1–2):71–81.
18. Ozer R. Inventor; E.I. Du Pont De Nemours And Company, assignee. Vapor phase decarbonylation process, US patent application US 2012/0165560 A1, 2012.
19. Jung KJ, Gaset A, Molinier J. Furfural decarbonylation catalyzed by charcoal supported palladium: Part I—Kinetics. *Biomass*. 1988; 16(1):63–76.
20. Jung KJ, Gaset A, Molinier J. Furfural decarbonylation catalyzed by charcoal supported palladium: Part II—A continuous process. *Biomass*. 1988;16(2):89–96.
21. Lohbeck K, Haferkorn H, Fuhrmann W, Fedtke N. Maleic and Fumaric Acids. *Ullmann's Encyclopedia of Industrial Chemistry*: Wiley-VCH Verlag GmbH, Weinheim, 2000.
22. Nielsen ER. Vapor phase oxidation of furfural. *Ind Eng Chem*. 1949; 41(2):365–368.
23. Slavinskaya VA, Kreile DR, Dzilyuma éE, Sile Dé. Incomplete catalytic oxidation of furan compounds (review). *Chem Heterocycl Compd* 1977;13(7):710–721.
24. Alonso-Fagúndez N, Granados ML, Mariscal R, Ojeda M. Selective conversion of furfural to maleic anhydride and furan with VOx/Al2O3 catalysts. *ChemSusChem*. 2012;5(10):1984–1990.
25. Rajamani K, Subramanian P, Murthy MS. Kinetics and mechanism of vapor phase oxidation of furfural over tin vanadate catalyst. *Ind Eng Chem Process Des Dev*. 1976;15(2):232–234.
26. Cherubini F, Strømman AH. Life cycle assessment of bioenergy systems: State of the art and future challenges. *Bioresour Technol* 2011; 102(2):437–451.
27. Kazi FK, Patel AD, Serrano-Ruiz JC, Dumesic JA, Anex RP. Techno-economic analysis of dimethylfuran (DMF) and hydroxymethylfurfural (HMF) production from pure fructose in catalytic processes. *Chem Eng J*. 2011;169(1–3):329–338.
28. Torres AI, Daoutidis P, Tsapatsis M. Continuous production of 5-hydroxymethylfurfural from fructose: a design case study. *Energy Environ Sci*. 2010;3(10):1560–1572.
29. Lin Z, Ierapetritou M, Nikolakis V. Aromatics from lignocellulosic biomass: economic analysis of the production of p-xylene from 5-hydroxymethylfurfural. *AIChE J*. 2013;59(6):2079–2087.
30. Lin Z, Nikolakis V, Ierapetritou M. Alternative approaches for p-xylene production from starch: techno-economic analysis. *Ind Eng Chem Res* 2014;53(26):10688–10699.
31. Han J, Sen SM, Alonso DM, Dumesic JA, Maravelias CT. A strategy for the simultaneous catalytic conversion of hemicellulose and cellulose from lignocellulosic biomass to liquid transportation fuels. *Green Chem*. 2014;16(2):653–661.
32. Lin Z, Nikolakis V, Ierapetritou M. Life cycle assessment of biobased p-xylene production. *Ind Eng Chem Res*. 2015;54(8):2366–2378.
33. OrbiChem T. Chemical Market Insight and Foresight—On a Single Page—Acetic anhydride. Available at http://www.orbichem.com/userfiles/CNF%20Samples/aca_13_11.pdf, 2013.
34. OrbiChem T. Chemical Market Insight and Foresight—On a Single Page—Acetic acid. Available at http://www.orbichem.com/userfiles/CNF%20Samples/acc_13_11.pdf, 2013.
35. Hosea Cheung, Robin S Tanke, G. Paul Torrence, Acetic Acid. *Ullmann's Encyclopedia of industrial chemistry*, VCH, Weinheim, 1985.
36. AspenTech. *Aspen Plus User Guide*: Aspen Technology Inc., Cambridge, MA, 2012.
37. Frenkel M, Chirico RD, Diky V, Yan X, Dong Q, Muzny C. ThermoData engine (TDE): software implementation of the dynamic data evaluation concept. *J Chem Inform Model*. 2005;45(4):816–838.
38. Chickos JS, Acree WE, Liebman JF. Estimating solid–liquid phase change enthalpies and entropies. *J Phys Chem Ref Data*. 1999;28(6): 1535–1673.
39. Goodman B, Wilding V, Oscarson J, Rowley R. Use of the DIPPR database for development of quantitative structure-property relationship correlations: heat capacity of solid organic compounds. *J Chem Eng Data* 2004;49:24–31.
40. McKetta JJ Jr. Volume 1—Abrasives to Acrylonitrile. *Encyclopedia of Chemical Processing and Design*, CRC Press, 1976.
41. AspenTech. *Aspen Icarus Reference Guide—Icarus Evaluation Engine (IEE) V8.0*: Aspen Technology Inc., 2012.
42. Hirshleifer J. On the theory of optimal investment decision. *J Pol Econ*. 1958;66(4):329–352.
43. Dutia P. Phthalic anhydride: a techno-commercial profile part 2: international scenario. *Chem Weekly*. Jan 8, 2008. 191–193, Available at http://www.chemicalweekly.com/Profiles/Phthalic_Anhydride_Part_2.pdf, accessed on August 24, 2014

44. Domtar. Mill Details. Available at http://www.domtar.com/en/paper-locations/paper-mill_marlboro.asp, accessed on May 17, 2015.
45. Milbrandt A. *A Geographic Perspective on the Current Biomass Resource Availability in the United States*: Golden, Colorado, National Renewable Energy Laboratory, 2005.
46. D. Humbird, R. Davis, L. Tao, C. Kinchin, D. Hsu, A. Aden, P. Schoen, J. Lukas, B. Olthof, M. Worley, D. Sexton,, and D. Dudgeon, Process Design and Economics for Biochemical Conversion of Lignocellulosic Biomass to Ethanol: *Dilute-Acid Pretreatment and Enzymatic Hydrolysis of Corn Stover*: Golden, Colorado, NREL, 2011.
47. R. Davis, L. Tao, E.C.D. Tan, M.J. Biddy, G.T. Beckham, C. Scarlata, J. Jacobson, K. Cafferty, J. Ross, J. Lukas, D. Knorr, and P. Schoen Process. Design and Economics for the Conversion of Lignocellulosic Biomass to Hydrocarbons: *Dilute-Acid and Enzymatic Deconstruction of Biomass to Sugars and Biological Conversion of Sugars to Hydrocarbons*: Golden, Colorado, NREL, 2013.
48. Natural Gas Weekly Update. Available at http://www.eia.gov/naturalgas/weekly/#tabs-prices-4, accessed on August 24, 2014.
49. BASF. Available at http://apps.catalysts.basf.com/apps/eibprices/mp, accessed on August 20, 2014.
50. Fung SC. Deactivation and regeneration/redispersion chemistry of Pt/KL-zeolite. In: Spivey JJ, Roberts GW Davis BH, editors. *Studies in Surface Science and Catalysis*. Vol 139, Elsevier, 2001:399–406. ISSN 0167-2991, ISBN 9780444504777, http://dx.doi.org/10.1016/S0167-2991(01)80223-8.
51. Jackson SD, Lennon D, Webb G, Willis J. Processes occurring during deactivation/regeneration of a vanadia/alumina catalyst under propane dehydrogenation conditions. In: Spivey JJ, Roberts GW, Davis BH, editors. *Studies in Surface Science and Catalysis*. Vol 139, Elsevier, 2001:271–278. ISSN 0167-2991, ISBN 9780444504777,
52. Royo C, Perdices JM, Monzón A, Santamaría J. Regeneration of fixed-bed catalytic reactors deactivated by coke: influence of operating conditions and of different pretreatments of the coke deposits. *Ind Eng Chem Res*. 1996;35(6):1813–1823.
53. Wooley RJ, Putsche V. *Development of an ASPEN PLUS Physical Property Database for Biofuels Components*, Golden, CO: National Renewable Energy Laboratory, 1996.
54. Pre. About SimaPro. Available at http://www.pre-sustainability.com/simapro-lca-software, accessed on May 20 2015.
55. The ecoinvent Database. Avaiable at http://www.ecoinvent.org/database/, accessed on July 16, 2014.
56. The ecoinvent Database v3.0. Available at https://ecoquery.ecoinvent.org/Details/UPR/EE7D4E1E-159C-4ABB-BF8D-0AA29C2D9210/DD7F13F5-0658-489C-A19C-F2FF8A00BDD9, accessed January 31, 2015.
57. Barre JC, Hofstetter P, Pennington DW, Haes HAUd. Life cycle impact assessment workshop summary—midpoints versus endpoints: the sacrifices and benefits. *Intl J Life Cycle Assessment*. 2000;5(6):319–326.
58. Rufford HJ, Inventor; Du Pont, assignee. Oxidation of 1,3 butadiene to furan, US patent US 2900396 A, 1959.
59. Tom A, Bither J, McClellan WR, Inventors; E. I. Du Pont De Nemours And Company, assignee. Preparation of furan, US patent US4322358 A, 1982.
60. Vernon R, Lindsey J, Prichard WW, Inventors; E.I. Du Pont De Nemours And Company, assignee. Catalytic conversion of butadiene to furan, EP0031729 B1, 1983.
61. Daniel R. Herrington APS, Inventor; The Standard Oil Company, assignee. Process for the manufacture of furan compounds, US patent US4323508 A, 1982.
62. Available at http://www.supplymanagement.com/news/2014/butadiene-price-rises-by-a-third, accessed on August 24, 2014.
63. Linde Engineering, Synthesis Gas. Available at http://www.linde-engineering.com/en/process_plants/hydrogen_and_synthesis_gas_plants/gas_products/synthesis_gas/index.html, accessed on May 20 2015.
64. Phthalic anhydride US. Available at http://www.icis.com/chemicals/phthalic-anhydride/us/?tab=tbc-tab2, accessed on July 2014.

Manuscript received Nov. 25, 2014, and revision received May 25, 2015.